Measurement of the B Meson Differential Cross Section $d\sigma/dp_T$ in $p\bar{p}$ Collisions at $\sqrt{s} = 1.8$ TeV

F. Abe,[13] M. G. Albrow,[7] S. R. Amendolia,[23] D. Amidei,[16] J. Antos,[28] C. Anway-Wiese,[4] G. Apollinari,[26] H. Areti,[7] M. Atac,[7] P. Auchincloss,[25] F. Azfar,[21] P. Azzi,[20] N. Bacchetta,[20] W. Badgett,[16] M. W. Bailey,[18] J. Bao,[35] P. de Barbaro,[25] A. Barbaro-Galtieri,[14] V. E. Barnes,[24] B. A. Barnett,[12] P. Bartalini,[23] G. Bauer,[15] T. Baumann,[9] F. Bedeschi,[23] S. Behrends,[3] S. Belforte,[23] G. Bellettini,[23] J. Bellinger,[34] D. Benjamin,[31] J. Benlloch,[15] J. Bensinger,[3] D. Benton,[21] A. Beretvas,[7] J. P. Berge,[7] S. Bertolucci,[8] A. Bhatti,[26] K. Biery,[11] M. Binkley,[7] F. Bird,[29] D. Bisello,[20] R. E. Blair,[1] C. Blocker,[3] A. Bodek,[25] W. Bokhari,[15] V. Bolognesi,[23] D. Bortoletto,[24] C. Boswell,[12] T. Boulos,[14] G. Brandenburg,[9] C. Bromberg,[17] E. Buckley-Geer,[7] H. S. Budd,[25] K. Burkett,[16] G. Busetto,[20] A. Byon-Wagner,[7] K. L. Byrum,[1] J. Cammerata,[12] C. Campagnari,[7] M. Campbell,[16] A. Caner,[7] W. Carithers,[14] D. Carlsmith,[34] A. Castro,[20] Y. Cen,[21] F. Cervelli,[23] H. Y. Chao,[28] J. Chapman,[16] M.-T. Cheng,[28] G. Chiarelli,[23] T. Chikamatsu,[32] C. N. Chiou,[28] L. Christofek,[10] S. Cihangir,[7] A. G. Clark,[23] M. Cobal,[23] M. Contreras,[5] J. Conway,[27] J. Cooper,[7] M. Cordelli,[8] C. Couyoumtzelis,[23] D. Crane,[1] J. D. Cunningham,[3] T. Daniels,[15] F. DeJongh,[7] S. Delchamps,[7] S. Dell'Agnello,[23] M. Dell'Orso,[23] L. Demortier,[26] B. Denby,[23] M. Deninno,[2] P. F. Derwent,[16] T. Devlin,[27] M. Dickson,[25] J. R. Dittmann,[6] S. Donati,[23] R. B. Drucker,[14] A. Dunn,[16] K. Einsweiler,[14] J. E. Elias,[7] R. Ely,[14] E. Engels, Jr.,[22] S. Eno,[5] D. Errede,[10] S. Errede,[10] Q. Fan,[25] B. Farhat,[15] I. Fiori,[2] B. Flaugher,[7] G. W. Foster,[7] M. Franklin,[9] M. Frautschi,[18] J. Freeman,[7] J. Friedman,[15] A. Fry,[29] T. A. Fuess,[1] Y. Fukui,[13] S. Funaki,[32] G. Gagliardi,[23] S. Galeotti,[23] M. Gallinaro,[20] A. F. Garfinkel,[24] S. Geer,[7] D. W. Gerdes,[16] P. Giannetti,[23] N. Giokaris,[26] P. Giromini,[8] L. Gladney,[21] D. Glenzinski,[12] M. Gold,[18] J. Gonzalez,[21] A. Gordon,[9] A. T. Goshaw,[6] K. Goulianos,[26] H. Grassmann,[6] A. Grewal,[21] L. Groer,[27] C. Grosso-Pilcher,[5] C. Haber,[14] S. R. Hahn,[7] R. Hamilton,[9] R. Handler,[34] R. M. Hans,[35] K. Hara,[32] B. Harral,[21] R. M. Harris,[7] S. A. Hauger,[6] J. Hauser,[4] C. Hawk,[27] J. Heinrich,[21] D. Cronin-Hennessy,[6] R. Hollebeek,[21] L. Holloway,[10] A. Hölscher,[11] S. Hong,[16] G. Houk,[21] P. Hu,[22] B. T. Huffman,[22] R. Hughes,[25] P. Hurst,[9] J. Huston,[17] J. Huth,[9] J. Hylen,[7] M. Incagli,[23] J. Incandela,[7] H. Iso,[32] H. Jensen,[7] C. P. Jessop,[9] U. Joshi,[7] R. W. Kadel,[14] E. Kajfasz,[7,*] T. Kamon,[30] T. Kaneko,[32] D. A. Kardelis,[10] H. Kasha,[35] Y. Kato,[19] L. Keeble,[8] R. D. Kennedy,[27] R. Kephart,[7] P. Kesten,[14] D. Kestenbaum,[9] R. M. Keup,[10] H. Keutelian,[7] F. Keyvan,[4] D. H. Kim,[7] H. S. Kim,[11] S. B. Kim,[16] S. H. Kim,[32] Y. K. Kim,[14] L. Kirsch,[3] P. Koehn,[25] K. Kondo,[32] J. Konigsberg,[9] S. Kopp,[5] K. Kordas,[11] W. Koska,[7] E. Kovacs,[7,*] W. Kowald,[6] M. Krasberg,[16] J. Kroll,[7] M. Kruse,[24] S. E. Kuhlmann,[1] E. Kuns,[27] A. T. Laasanen,[24] N. Labanca,[23] S. Lammel,[4] J. I. Lamoureux,[3] T. LeCompte,[10] S. Leone,[23] J. D. Lewis,[7] P. Limon,[7] M. Lindgren,[4] T. M. Liss,[10] N. Lockyer,[21] C. Loomis,[27] O. Long,[21] M. Loreti,[20] E. H. Low,[21] J. Lu,[30] D. Lucchesi,[23] C. B. Luchini,[10] P. Lukens,[7] J. Lys,[14] P. Maas,[34] K. Maeshima,[7] A. Maghakian,[26] P. Maksimovic,[15] M. Mangano,[23] J. Mansour,[17] M. Mariotti,[20] J. P. Marriner,[7] A. Martin,[10] J. A. J. Matthews,[18] R. Mattingly,[15] P. McIntyre,[30] P. Melese,[26] A. Menzione,[23] E. Meschi,[23] G. Michail,[9] S. Mikamo,[13] M. Miller,[5] R. Miller,[17] T. Mimashi,[32] S. Miscetti,[8] M. Mishina,[13] H. Mitsushio,[32] S. Miyashita,[32] Y. Morita,[23] S. Moulding,[26] J. Mueller,[27] A. Mukherjee,[7] T. Muller,[4] P. Musgrave,[11] L. F. Nakae,[29] I. Nakano,[32] C. Nelson,[7] D. Neuberger,[4] C. Newman-Holmes,[7] L. Nodulman,[1] S. Ogawa,[32] S. H. Oh,[6] K. E. Ohl,[35] R. Oishi,[32] T. Okusawa,[19] C. Pagliarone,[23] R. Paoletti,[23] V. Papadimitriou,[31] S. Park,[7] J. Patrick,[7] G. Pauletta,[23] M. Paulini,[14] L. Pescara,[20] M. D. Peters,[14] T. J. Phillips,[6] G. Piacentino,[2] M. Pillai,[25] R. Plunkett,[7] L. Pondrom,[34] N. Produit,[14] J. Proudfoot,[1] F. Ptohos,[9] G. Punzi,[23] K. Ragan,[11] F. Rimondi,[2] L. Ristori,[23] M. Roach-Bellino,[33] W. J. Robertson,[6] T. Rodrigo,[7] J. Romano,[5] L. Rosenson,[15] W. K. Sakumoto,[25] D. Saltzberg,[5] A. Sansoni,[8] V. Scarpine,[30] A. Schindler,[14] P. Schlabach,[9] E. E. Schmidt,[7] M. P. Schmidt,[35] O. Schneider,[14] G. F. Sciacca,[23] A. Scribano,[23] S. Segler,[7] S. Seidel,[18] Y. Seiya,[32] G. Sganos,[11] A. Sgolacchia,[2] M. Shapiro,[14] N. M. Shaw,[24] Q. Shen,[24] P. F. Shepard,[22] M. Shimojima,[32] M. Shochet,[5] J. Siegrist,[29] A. Sill,[31] P. Sinervo,[11] P. Singh,[22] J. Skarha,[12] K. Sliwa,[33] D. A. Smith,[23] F. D. Snider,[12] L. Song,[7] T. Song,[16] J. Spalding,[7] L. Spiegel,[7] P. Sphicas,[15] A. Spies,[12] L. Stanco,[20] J. Steele,[34] A. Stefanini,[23] K. Strahl,[11] J. Strait,[7] D. Stuart,[7] G. Sullivan,[5] K. Sumorok,[15] R. L. Swartz, Jr.,[10] T. Takahashi,[19] K. Takikawa,[32] F. Tartarelli,[23] W. Taylor,[11] P. K. Teng,[28] Y. Teramoto,[19] S. Tether,[15] D. Theriot,[7] J. Thomas,[29] T. L. Thomas,[18] R. Thun,[16] M. Timko,[33] P. Tipton,[25] A. Titov,[26] S. Tkaczyk,[7] K. Tollefson,[25] A. Tollestrup,[7] J. Tonnison,[24] J. F. de Troconiz,[9] J. Tseng,[12] M. Turcotte,[29] N. Turini,[23] N. Uemura,[32] F. Ukegawa,[21] G. Unal,[21] S. C. van den Brink,[22] S. Vejcik III,[16] R. Vidal,[7] M. Vondracek,[10] D. Vucinic,[15] R. G. Wagner,[1] R. L. Wagner,[7] N. Wainer,[7] R. C. Walker,[25] C. Wang,[6] C. H. Wang,[28] G. Wang,[23] J. Wang,[5] M. J. Wang,[28] Q. F. Wang,[26] A. Warburton,[11] G. Watts,[25] T. Watts,[27] R. Webb,[30] C. Wei,[6]

C. Wendt,[34] H. Wenzel,[14] W. C. Wester III,[7] T. Westhusing,[10] A. B. Wicklund,[1] E. Wicklund,[7] R. Wilkinson,[21]
H. H. Williams,[21] P. Wilson,[5] B. L. Winer,[25] J. Wolinski,[30] D. Y. Wu,[16] X. Wu,[23] J. Wyss,[20] A. Yagil,[7] W. Yao,[14]
K. Yasuoka,[32] Y. Ye,[11] G. P. Yeh,[7] P. Yeh,[28] M. Yin,[6] J. Yoh,[7] C. Yosef,[17] T. Yoshida,[19] D. Yovanovitch,[7] I. Yu,[35]
J. C. Yun,[7] A. Zanetti,[23] F. Zetti,[23] L. Zhang,[34] S. Zhang,[16] W. Zhang,[21] and S. Zucchelli[2]

(CDF Collaboration)

[1]Argonne National Laboratory, Argonne, Illinois 60439
[2]Istituto Nazionale di Fisica Nucleare, University of Bologna, I-40126 Bologna, Italy
[3]Brandeis University, Waltham, Massachusetts 02254
[4]University of California at Los Angeles, Los Angeles, California 90024
[5]University of Chicago, Chicago, Illinois 60637
[6]Duke University, Durham, North Carolina 27708
[7]Fermi National Accelerator Laboratory, Batavia, Illinois 60510
[8]Laboratori Nazionali di Frascati, Istituto Nazionale di Fisica Nucleare, I-00044 Frascati, Italy
[9]Harvard University, Cambridge, Massachusetts 02138
[10]University of Illinois, Urbana, Illinois 61801
[11]Institute of Particle Physics, McGill University, Montreal, Canada H3A 2T8
and University of Toronto, Toronto, Canada M5S 1A7
[12]The Johns Hopkins University, Baltimore, Maryland 21218
[13]National Laboratory for High Energy Physics (KEK), Tsukuba, Ibaraki 305, Japan
[14]Lawrence Berkeley Laboratory, Berkeley, California 94720
[15]Massachusetts Institute of Technology, Cambridge, Massachusetts 02139
[16]University of Michigan, Ann Arbor, Michigan 48109
[17]Michigan State University, East Lansing, Michigan 48824
[18]University of New Mexico, Albuquerque, New Mexico 87131
[19]Osaka City University, Osaka 588, Japan
[20]Università di Padova, Istituto Nazionale di Fisica Nucleare, Sezione di Padova, I-35131 Padova, Italy
[21]University of Pennsylvania, Philadelphia, Pennsylvania 19104
[22]University of Pittsburgh, Pittsburgh, Pennsylvania 15260
[23]Istituto Nazionale di Fisica Nucleare, University and Scuola Normale Superiore of Pisa, I-56100 Pisa, Italy
[24]Purdue University, West Lafayette, Indiana 47907
[25]University of Rochester, Rochester, New York 14627
[26]Rockefeller University, New York, New York 10021
[27]Rutgers University, Piscataway, New Jersey 08854
[28]Academia Sinica, Taiwan 11529, Republic of China
[29]Superconducting Super Collider Laboratory, Dallas, Texas 75237
[30]Texas A&M University, College Station, Texas 77843
[31]Texas Tech University, Lubbock, Texas 79409
[32]University of Tsukuba, Tsukuba, Ibaraki 305, Japan
[33]Tufts University, Medford, Massachusetts 02155
[34]University of Wisconsin, Madison, Wisconsin 53706
[35]Yale University, New Haven, Connecticut 06511
(Received 21 March 1995)

This paper presents the first direct measurement of the B meson differential cross section $d\sigma/dp_T$ in $p\bar{p}$ collisions at $\sqrt{s} = 1.8$ TeV using a sample of 19.3 ± 0.7 pb^{-1} accumulated by the Collider Detector at Fermilab. The cross section is measured in the central rapidity region $|y| < 1$ for $p_T(B) > 6.0$ GeV/c by fully reconstructing the B meson decays $B^+ \rightarrow J/\psi K^+$ and $B^0 \rightarrow J/\psi K^{*0}(892)$, where $J/\psi \rightarrow \mu^+\mu^-$ and $K^{*0} \rightarrow K^+\pi^-$. A comparison is made to the theoretical QCD prediction calculated at next-to-leading order.

The prediction of QCD theory was in agreement with the first b quark cross section measurements in $p\bar{p}$ collisions which were made by UA1 at $\sqrt{s} = 630$ GeV [1]. Initial measurements made at $\sqrt{s} = 1.8$ TeV at the Collider Detector at Fermilab (CDF) [2–4] cast doubt on whether QCD correctly predicts either the absolute rate or shape of the transverse momentum (p_T) distribution, whereas, a measurement made more recently at the D0

detector [5] at the same center-of-mass energy is in agreement with the QCD prediction. We present the first direct measurement of the B meson differential cross section $d\sigma/dp_T$ in hadronic collisions by measuring the mass and momentum of the B meson decaying into exclusive final states. The differential cross section so obtained provides a test of the QCD prediction that is complementary to measurements which infer the b quark content

and momentum distribution from an inclusive lepton spectrum after unfolding contributions from both b and c quarks. The data sample used represents 19.3 ± 0.7 pb^{-1} collected by CDF during the 1992–93 run. B mesons are reconstructed via the decays $B^+ \rightarrow J/\psi K^+$ and $B^0 \rightarrow J/\psi K^{*0}(892)$, with $J/\psi \rightarrow \mu^+ \mu^-$ and $K^{*0} \rightarrow K^+ \pi^-$ and their charge conjugates.

Detailed descriptions of the CDF detector have been provided elsewhere [6]. The components relevant to this analysis are briefly described here. The z axis of the detector coordinate system is along the beam direction. The central tracking chamber (CTC) is a drift chamber in a 1.4 T axial magnetic field, consisting of nine superlayers, four of which give stereo information. A particle must have pseudorapidity $|\eta| < 1$ to pass through all nine superlayers, which defines the rapidity range used for the cross-section measurement.

A silicon vertex detector (SVX) provides high-resolution r-ϕ tracking information near the interaction region [7]. The SVX detector is 51 cm long and consists of four layers of silicon microstrip detectors with an innermost radius of 2.9 cm. Pattern recognition is done by extrapolating tracks from the CTC. The longitudinal distribution of the primary vertices is such that SVX information is available for about 60% of all tracks. If SVX information is added to a track, the momentum resolution $\delta p_T / p_T$ improves from $\sim 0.002 p_T$ to $[(0.0009 p_T)^2 + (0.0066)^2]^{1/2}$, where p_T is measured in GeV/c. Surrounding the CTC are electromagnetic and hadronic calorimeters, outside of which are the central muon chambers, segmented into 72 modules which provide about 85% coverage in azimuth in the pseudorapidity range $|\eta| < 0.6$.

The selection of B candidates begins by identifying J/ψ candidates that decay to two muons. There are three levels of trigger requirements that must be satisfied for a muon pair to be included in the J/ψ data sample. At the first trigger level, the muons must have been detected in the central muon chambers and pass a minimal transverse momentum requirement of ~ 1.4 GeV/c. Prompt muons with lower momenta range out in the calorimeters. The efficiency for this trigger is 90% at $p_T = 3.1$ GeV/c. At the second trigger level, at least one of the muon-chamber tracks must match a track found in the CTC by a hardware track processor. The efficiency for the track processor rises from 10% at 2.3 GeV/c to 90% at 3.1 GeV/c. At the third (software) trigger level, detailed CTC pattern recognition and tracking are done, and the dimuon invariant mass is required to be within 300 MeV/c^2 of the J/ψ mass.

To improve the purity of the J/ψ sample, the CTC track is required to match its associated muon chamber track to within 3σ in r-ϕ and 3.5σ in z. To match the trigger thresholds, each muon is required to have $p_T \geq 1.8$ GeV/c, and at least one muon is required to have $p_T \geq 2.8$ GeV/c. The invariant mass and uncertainty σ_m are calculated for each muon pair. A fit to the mass

distribution indicates about 45 000 J/ψ over background. The signal region is defined to be those dimuon candidates with invariant masses within $4\sigma_m$ of the known J/ψ mass [8]. The K^+ and K^{*0} candidates are required to have $p_T > 1.25$ GeV/c; furthermore, each K^{*0} decay product is required to have $p_T > 400$ MeV/c to ensure reliable tracking. All pairs of oppositely charged particle tracks are considered to be candidates for the K^{*0} decay products. The $K\pi$ invariant mass is required to be within 50 MeV/c^2 of the K^{*0} mass. Unlike combinatoric background, the invariant mass reconstructed for an actual B^0 meson peaks at the B^0 mass when the kaon and pion mass assignments are exchanged. To avoid double counting, only the K^{*0} candidate with the mass closest to the K^{*0} mass is used.

We find the B-candidate mass and momentum subject to the constraint that the decay tracks come from a common vertex and the invariant mass of the dimuon tracks is equal to the J/ψ mass. We require the confidence level of the fit to be greater than 0.5%. The transverse momentum for each B candidate is required to be greater than 6.0 GeV/c, the minimum p_T required to produce decay products satisfying the trigger and selection requirements. The proper decay length $c\tau \equiv L_{xy} m_B / p_T$ is calculated, where L_{xy} is the projection of the B vertex displacement onto the B transverse momentum. About 75% of the background that occurs when a prompt J/ψ is combined with other tracks from the primary vertex is removed by requiring $c\tau$ to be greater than 100 μm.

The B candidates are divided into subsamples in p_T ranges 6–9, 9–12, 12–15, and >15 GeV/c. Isospin symmetry in fragmentation, i.e., equal production of B^+ and B^0, is expected to hold for central production [9]. To make the best measurement of $d\sigma/dp_T$, the charged and neutral data samples are combined to determine the average B meson cross section. For each p_T range, the invariant mass distributions are fit simultaneously, using an unbinned likelihood method. The relative numbers of signal events for each p_T bin are constrained to be proportional to the relative reconstruction efficiencies $\epsilon(B^0)/\epsilon(B^+)$, which are shown in Table I. The mass is set to 5.274 GeV/c, which is the value found from a fit to the entire data sample. The mass range below 5.2 GeV/c^2 is excluded from the fit since it can include contributions from higher multiplicity B decay modes. We find that the background is well represented by events which are likely to contain B mesons displaced from the primary vertex because they fail the vertex χ^2 confidence level cut. The background slope in the fit is constrained to equal the slope determined from such events. The invariant mass distributions for each momentum range are shown in Fig. 1. The total number of B mesons determined from the simultaneous fit method $N(B)$ is given in Table I, along with the fitted number of events found from the charged sample alone $N(B^{\pm})$. The systematic uncertainty in the fitting method is determined to be 9.2% by taking into account the uncertainties in the mass, background slopes, and relative reconstruction efficiencies.

TABLE I. B meson differential cross section $d\sigma(|y| < 1.0)/dp_T$ [nb/(GeV/c)]. The uncertainty listed for the relative reconstruction efficiency $\epsilon(B^0)/\epsilon(B^+)$ includes the branching ratio uncertainty. The fitted numbers of events, denoted by $N(B^\pm)$ for the charged meson sample and $N(B)$ for the combined charged and neutral meson sample, include both B and $\bar{B}$ mesons, while the corresponding cross sections are for B mesons only. The uncertainties shown for the number of events are statistical only.

$\langle p_T \rangle$ (GeV/c)	Acceptance for B^+ (%)	$\epsilon(B^0)/\epsilon(B^+)$	$N(B^\pm)$	$d\sigma(B^+)/dp_T$ [nb/(GeV/c)]			$N(B)$	$d\sigma(B)/dp_T$ [nb/(GeV/c)]		
7.4	1.28 ± 0.01	0.52 ± 0.12	51 ± 10	644	± 126	± 139	72 ± 12	596	± 103	± 106
10.4	3.71 ± 0.04	0.58 ± 0.14	31 ± 7	134	± 30	± 29	42 ± 9	116	± 24	± 21
13.4	6.45 ± 0.06	0.61 ± 0.15	20 ± 5	50	± 13	± 11	35 ± 7	55	± 10	± 10
20.0	9.55 ± 0.10	0.71 ± 0.17	24 ± 4	9.5 ±	1.6 ±	2.6	31 ± 6	7.2 ±	1.4 ±	1.8

The B-meson differential cross section is calculated from

$$\frac{d\sigma(B)}{dp_T} = \frac{N}{2\mathcal{L} A \epsilon F \Delta p_T}, \qquad (1)$$

where N is the number of events observed, $\mathcal{L}$ is the integrated luminosity, A is the detector acceptance (including the efficiency of the kinematic cuts), ϵ is the combined tracking and track-matching efficiency, F is the branching fraction, and Δp_T is the width of the p_T bin. The factor of $\frac{1}{2}$ is included because decays involving both B and $\bar{B}$ mesons have been reconstructed, but the quoted cross sections are for B mesons only.

A Monte Carlo simulation employing the next-to-leading order QCD calculation [10] with renormalization scale $\mu_0 = \sqrt{m_b^2 + p_T^2}$, where the b-quark mass m_b is equal to 4.75 GeV/c^2, the MRSD$_0$ proton parton distribution functions [11], the Peterson parametrization [12] for fragmentation, using a value of the fragmentation parameter of 0.006, and a detector and J/ψ trigger
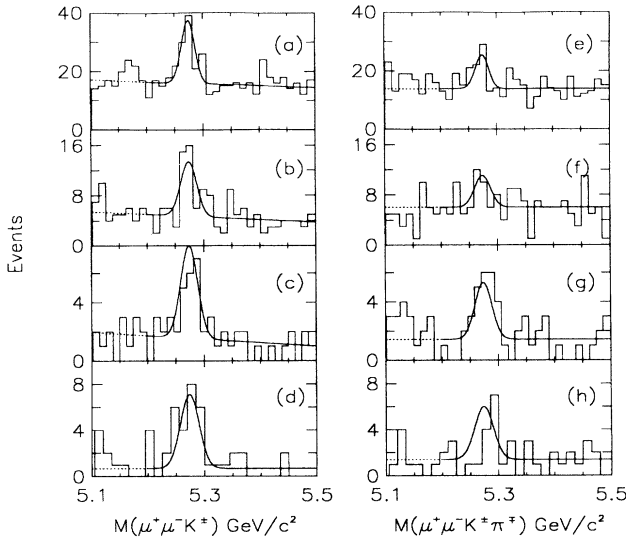

FIG. 1. $B^\pm$ and B^0 meson invariant mass distributions for the momentum ranges (a),(e) 6–9 GeV/c, (b),(f) 9–12 GeV/c, (c),(g) 12–15 GeV/c, and (d),(h) >15 GeV/c. The bin width is 15 MeV/c^2 for (d) and (h), and 12 MeV/c^2 for the remaining figures.

simulation was used to determine the acceptance, shown in Table I.

On-line (third trigger level) and off-line tracking efficiencies are (97 ± 2)% and (98.5 ± 1.4)%, respectively. The efficiency of the matching requirement between the CTC track and the muon chamber track segment is (98.7 ± 1)%. Product branching fractions of (6.55 ± 1.01) × 10^{-5} and (6.67 ± 1.21) × 10^{-5} [13] were used for the $B^+ \to J/\psi K^+$ and $B^0 \to J/\psi K^{*0}$ decays, which include the $J/\psi \to \mu^+\mu^-$ and $K^{*0} \to K^+\pi^-$ branching ratios. These branching ratios are included in the relative reconstruction efficiencies given in Table I.

Varying the b quark mass and the QCD renormalization scale used in the Monte Carlo simulation within their uncertainties changes the calculated acceptance by ±2% [14]. The systematic uncertainty in the J/ψ efficiency due to the trigger parametrization was determined to be 5.5%. Additionally, a systematic uncertainty of 4% is associated with the reconstruction of kaons that decay inside the CTC volume. The efficiency of the 100 μm cut on $c\tau$ has an uncertainty of 4%, due to its dependence on the lifetime of the meson and the $c\tau$ resolution [14], which varies from 50 to 300 μm, depending on whether or not SVX information was available for the vertex fit. The χ^2 requirement on the common-vertex constraint has an additional 1% uncertainty, which was determined from the fraction of J/ψ that fail such a requirement. Varying the polarization of the $B^0 \to J/\psi K^{*0}$ decay products in the range (80 ± 10)% [15] changes the calculated acceptance by ±5.7%. The total reconstruction efficiencies are (81.3 ± 9.1)% for the B^+ decay and (79.9 ± 10.8)% for the B^0 decay.

The average B meson cross-section results $d\sigma(B)/dp_T$ are listed in Table I and plotted in Fig. 2, where the common branching ratio uncertainty of 11.9% (included in Table I) is shown separately. For comparison, the cross section found from the charged data sample alone $d\sigma(B^+)/dp_T$ is also given in Table I. The differential cross-section measurement at 20 GeV/c is obtained by dividing the integrated cross section above 15 GeV/c by an effective bin width determined from the data to be 12.7 ± 1.3 GeV/c. The point is plotted at the mean p_T value of the data points. The integrated cross section above 6 GeV/c is 2.39 ± 0.32 ± 0.44 μb. The solid curve in Fig. 2 shows the B meson differential
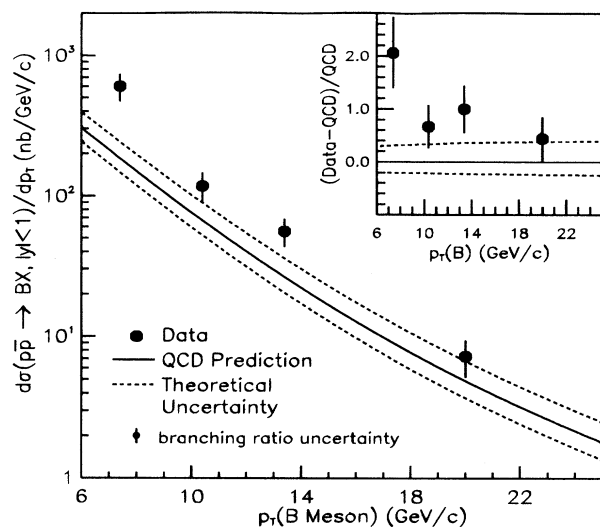
FIG. 2.   Average B meson differential cross section compared to the QCD-based Monte Carlo simulation described in the text. The branching ratio uncertainty, which contributes 11.9% to the cross-section uncertainty, is shown separately. The dashed curves indicate the uncertainty in the theoretical prediction. The inset plot shows (data-QCD)/QCD on a linear scale.

cross section predicted by the QCD-based Monte Carlo simulation as described above, while the dashed curves indicate the variation associated with uncertainty in the b quark mass, the fragmentation parameter, and the renormalization scale [16]. The curves include the generally used assumption that 75% of $\bar{b}$ quarks fragment in equal amounts to B^+ and B^0 mesons [3,17]. The visual comparison between data and theory is aided by plotting (data-QCD)/QCD on a linear scale, as shown in the inset to Fig. 2. To determine the level of agreement between the data and the theoretical prediction, the predicted cross section is fitted to the measurements, holding the shape constant and varying the magnitude. The fit yields an overall scale factor of 1.9 $\pm$ 0.2 $\pm$ 0.2, with a confidence level of 20%. In conclusion, we find that the shape of the B meson differential cross section presented here is adequately described by next-to-leading order QCD, while the absolute rate is at the limits of that predicted by typical variations in the theoretical parameters. It will be interesting to compare these data to higher order calculations as they become available.

*Visitor.
[1] UA1 Collaboration, C. Albajar et al., Phys. Lett. B **186**, 237 (1987); **213**, 405 (1988); **256**, 121 (1991).
[2] CDF Collaboration, F. Abe et al., Phys. Rev. Lett. **71**, 500 (1993); **71**, 2396 (1993); Report No. Fermilab-Pub-94/131-E (to be published).
[3] CDF Collaboration, F. Abe et al., Phys. Rev. Lett. **68**, 3403 (1992); Phys. Rev. D **50**, 4252 (1994).
[4] CDF Collaboration, F. Abe et al., Phys. Rev. Lett. **69**, 3704 (1992); **71**, 2537 (1993). These papers assumed no direct production of J/ψ or $\psi(2S)$.
[5] D0 Collaboration, S. Abachi et al., Phys. Rev. Lett. **74**, 3548 (1995).
[6] CDF Collaboration, F. Abe et al., Nucl. Instrum. Methods Phys. Res., Sect. A **271**, 387 (1988).
[7] D. Amidei et al., Nucl. Instrum. Methods Phys. Res., Sect. A **350**, 73 (1994).
[8] M. Aguilar-Benitez et al., Phys. Rev. D **50**, 1173 (1994).
[9] I. Dunietz and J. Rosner, Report No. Fermilab-Pub-94/298-T.
[10] P. Dawson et al., Nucl. Phys. **B327**, 49 (1988); M. Mangano et al., Nucl. Phys. **B373**, 295 (1992).
[11] A. Martin, R. Roberts, and J. Stirling, Phys. Rev. D **47**, 867 (1993).
[12] C. Peterson et al., Phys. Rev. D **27**, 105 (1983); J. Chrin, Z. Phys. C **36**, 163 (1987).
[13] CLEO Collaboration, M. S. Alam et al., Phys. Rev. D **50**, 43 (1994).
[14] M. W. Bailey, Ph.D. thesis, Purdue University, 1994.
[15] CLEO Collaboration, M. S. Alam et al., Phys. Rev. D **50**, 43 (1994); ARGUS Collaboration, H. Albrecht et al., Phys. Lett. B **340**, 217 (1994); CDF Collaboration, F. Abe et al., Report No. Fermilab-Conf-94/216-E.
[16] The b quark mass is varied between 4.5 and 5.0 GeV/c, the renormalization scale is varied between $\mu_0/2$ and $2\mu_0$, and the fragmentation parameter is varied between 0.004 and 0.008.
[17] L3 Collaboration, B. Adeva et al., Phys. Lett. B **252**, 703 (1990); ALEPH Collaboration, D. Decamp et al., Phys. Lett. B **258**, 236 (1991); UA1 Collaboration, H. C. Albajar et al., Phys. Lett. B **262**, 171 (1991); CDF Collaboration, F. Abe et al., Phys. Rev. Lett. **67**, 3351 (1991).